

Nonreciprocal Bandpass Filter Using Mixed Static and Time-Modulated Resonators

Girdhari Chaudhary^{id}, *Member, IEEE*, and Yongchae Jeong^{id}, *Senior Member, IEEE*

Abstract—This letter presents a magnet-less nonreciprocal bandpass filter (BPF) that uses coupled static and time-modulated resonators. This coupling allows the nonreciprocal BPF to achieve minimum forward insertion loss (IL) and two pole isolation within the passband and shows wideband and high isolation. The modulation signal is directly applied to the varactor through the transmission line. This design, while simple, nevertheless achieves an excellent nonreciprocal response. We designed, simulated, and experimentally validated a microstrip line nonreciprocal BPF at 1.46 GHz. The results achieved in experiment were consistent with those obtained through simulations; forward IL of 3.10 dB and reverse isolation of 20 dB over a bandwidth of 50 MHz.

Index Terms—Bandpass filter (BPF), mixed resonators, nonreciprocal, spatio-temporal modulation, time-modulated resonators.

I. INTRODUCTION

NONRECIPROCAL components, such as circulators and isolators, are crucial to modern wireless communication systems [1]–[3]. These components are traditionally almost entirely based on the magnetic biasing of rare-earth ferrite materials [4], [5]. Some researchers have attempted to develop active and nonlinear circuits capable of achieving nonreciprocity without the use of a magnet. Typically, however, these approaches suffer from a poor noise figure and limited power handling capability [6], [7].

Magnet-less nonreciprocal bandpass filters (BPFs) that use time-modulated resonators to permit a signal to travel in only one direction ($|S_{21}| \neq |S_{12}|$) have been reported by a number of research teams [8]–[18]. To achieve practical RF filtering performances with a satisfactory forward insertion loss (IL), return loss (RL), and backward isolation with two poles, most researchers have employed at least three time-modulated resonators with a progressive phase shift, a design that increases modulation signal circuit complexity [11]–[15]. Wu *et al.* [16], [17] reported a microstrip line nonreciprocal BPF that employed only two time-modulated resonators, though the RF performances were inferior in terms of forward IL (>5.5 dB) and backward isolation (<9.8 dB with single pole).

In this letter, we propose a nonreciprocal BPF that uses coupled static and time-modulated resonators. Static resonators,

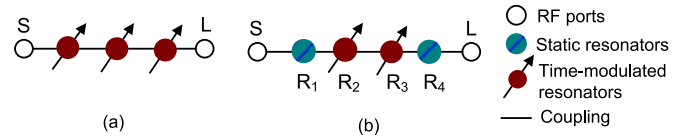


Fig. 1. Coupling diagram of magnet-less nonreciprocal BPF. (a) Conventional nonreciprocal BPF using three time-modulated resonators [11]–[15]. (b) Proposed nonreciprocal BPF using mixed static and time-modulated resonators.

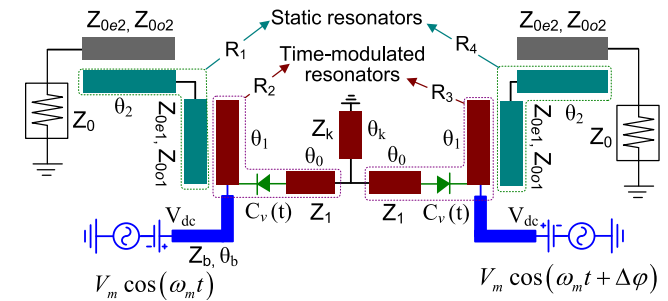


Fig. 2. TL model of proposed nonreciprocal BPF.

when properly coupled to time modulated resonators, creates two poles of reverse isolation, which increase the nonreciprocity isolation bandwidth (BW). The proposed coupling of static and time-modulated resonators simplifies modulation signal circuit design by decreasing the number of time-modulated resonators necessary to achieve high and wideband reverse isolation.

II. DESIGN THEORY

Fig. 1 shows the coupling diagrams of conventional and the proposed nonreciprocal BPFs. The coupling diagram of the proposed nonreciprocal BPF shown in Fig. 1(b) consists of RF ports, two static resonators (R_1 and R_4), and two spatio-temporally modulated (STM) time-varying resonators (R_2 and R_3). To achieve a magnet-less non-reciprocal BPF ($|S_{21}| \neq |S_{12}|$) based on STM, the resonators (R_2 and R_3) are modulated in time and space by modulating the capacitors as follows:

$$C_v(t) = C_0 + \Delta C \cos(2\pi f_m t + \Delta\phi) \quad (1)$$

where C_0 , ΔC , f_m , and $\Delta\phi$ are nominal capacitance, modulation depth, modulation frequency, and progressive phase shift of the modulation signal, respectively [11]. When proper modulation parameters (ΔC , f_m , $\Delta\phi$) are used, the powers at intermodulation products can be constructively collected at the RF carrier frequency to provide a small forward transmission loss or destructively added up in the reverse direction to create high isolation.

Fig. 2 shows the microstrip line schematic of the proposed nonreciprocal BPF. The time-modulated resonators

Manuscript received September 29, 2021; accepted October 22, 2021. Date of publication November 8, 2021; date of current version April 8, 2022. This work was supported in part by the National Research Foundation of Korea (NRF) grant funded by Korea Government (MSIT) under Grant 2020R1A2C2C012057 and in part by the NRF of Korea through the Basic Science Research Program funded by the Ministry of Education under Grant 2019R1A6A1A09031717. (Corresponding author: Yongchae Jeong.)

The authors are with the Division of Electronics and Information Engineering, IT Convergence Research Center, Jeonbuk National University, Jeonju-si 54896, South Korea (e-mail: girdharic@jbnu.ac.kr; ycjeong@jbnu.ac.kr).

Color versions of one or more figures in this letter are available at <https://doi.org/10.1109/LMWC.2021.3123306>.

Digital Object Identifier 10.1109/LMWC.2021.3123306

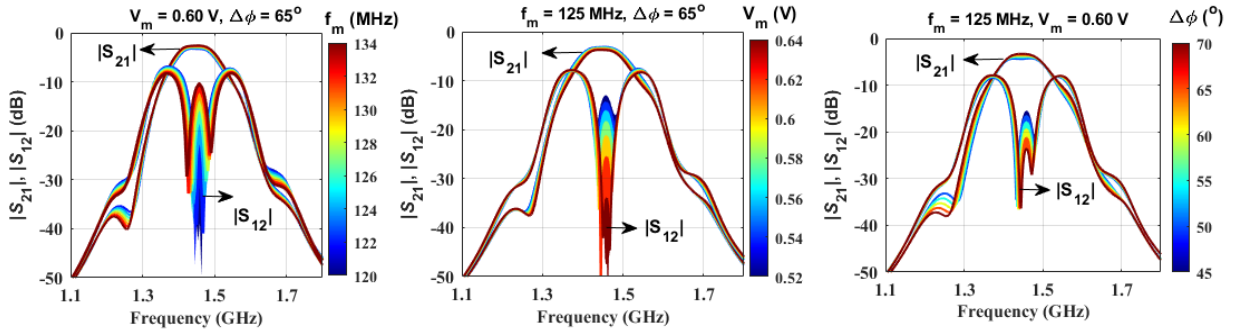


Fig. 3. Simulation results of forward IL and reverse isolation according to modulation parameters (f_m , V_m , and $\Delta\phi$).

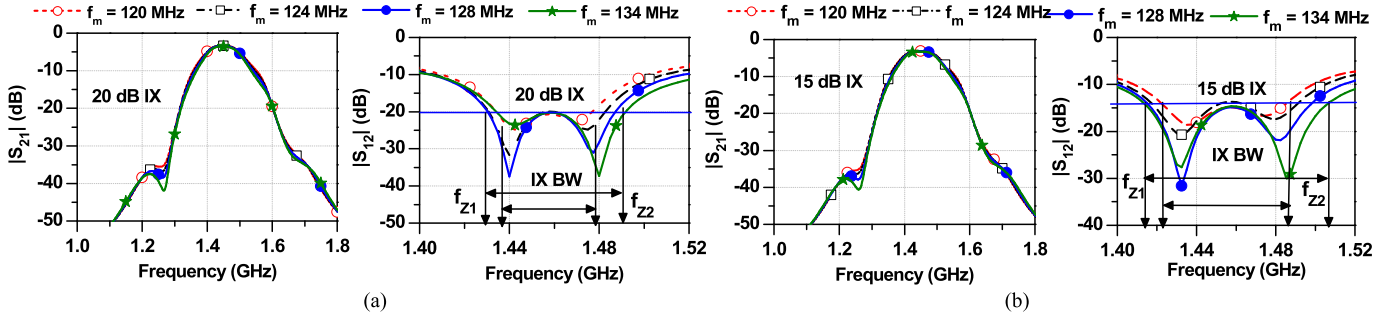


Fig. 4. Simulation results of forward IL and reverse isolation (IX) according to modulating frequency. (a) 20 dB IX and (b) 15 dB IX BW.

TABLE I

CIRCUIT PARAMETERS OF PROPOSED MICROSTRIP LINE NONRECIPROCAL BPF. ELECTRICAL LENGTHS ARE DEFINED AT 1.5 GHz

Z_1 (Ω)	Z_k (Ω)	θ_0	θ_1	θ_2	θ_k
50	50	17.97°	90°	94.6°	2.10°
Z_{0e1} (Ω)	Z_{0o1} (Ω)	Z_{0e2} (Ω)	Z_{0o2} (Ω)	Z_b (Ω)	θ_b
53.27	47.10	68.91	39.60	90	80°
$C_v = 6.90$ pF		Varactor: SMV 1233-079 from Sky works			

(R_2 and R_3) are realized by using quarter-wavelength transmission line (TL) loaded with varactor. The static resonators R_1 and R_4 are coupled to time-modulated resonators R_2 and R_3 through a parallel coupled line with even- and odd-mode impedances of Z_{0e1} and Z_{0o1} . Time-modulated resonators R_2 and R_3 are likewise coupled through a T-type short-circuited TL with characteristic impedance of Z_k and electrical length θ_k . Finally, the RF ports are coupled with a static resonator through parallel coupled line with even- and odd-mode impedances of Z_{0e2} and Z_{0o2} . The modulation signal and dc bias voltage are applied to time-varying resonators through the TL with a characteristic impedance of Z_b and electrical length θ_b , simplifying the biasing and modulation circuit.

A. Parametric Simulation for Proper Selection of Modulation Parameters

The proposed nonreciprocal BPF is designed for a 0.043-dB Chebyshev response (passband RL = 20 dB) with a center frequency of 1.46 GHz and a static equiripple BW (BW_r) of 130 MHz. The circuit parameters of filter, as calculated using filter theory, are given in Table I.

To overcome the complexity associated with analytical calculation of the appropriate modulation parameters that allow for nonreciprocal filtering response [11], we performed parametric studies of modulation parameters (f_m , V_m , $\Delta\phi$). These

were performed using a varactor SMV-1233 SPICE model manufactured by Skyworks [19]. The time-varying capacitors were implemented with reverse biased varactor diodes. Bias voltage $V_{dc} = 1.60$ V is provided for each varactor to set the nominal capacitance of 6.90 pF.

Fig. 3 shows the simulated results of the proposed nonreciprocal BPF. The proposed filter exhibits nonreciprocal BPF response during various combinations of f_m , $\Delta\phi$, and V_m . The BPF exhibits two poles in reverse isolation ($|S_{12}|$). Similarly, when f_m is slightly higher than the equiripple BW (e.g., 130 MHz), the BW of the reverse isolation increased, though isolation magnitude at f_0 decreased. Likewise, a large V_m exhibits high backward isolation, but the forward IL and RL slightly degraded. The proposed BPF exhibits strong reverse isolation when $\Delta\phi$ is between 45° and 70°.

Fig. 4 shows the simulation results of the proposed nonreciprocal BPF by maintaining reverse isolation (IX) of 20 dB and 15 dB at f_0 . The IX BW is slightly improved by increasing f_m ; however, forward IL is slightly degraded.

Fig. 5 shows 3-dB forward IL and backward reverse IX BWs according to f_m and V_m . The 3-dB forward IL BW is wider for lower f_m ; however, IX BW is narrower. The highest 20-dB IX BW is achieved when $f_m = 128$ MHz. Similarly, highest 15-dB IX BW is achieved when $f_m = 134$ MHz.

Fig. 6 shows the simulation results of nonreciprocal BPF with and without static resonators. Two distinct poles in reverse isolation are observed in case of mixed static and time-modulated resonators, providing the wideband and high reverse isolation without increasing number of modulation signals.

III. SIMULATION AND MEASUREMENT RESULTS

To experimentally validate the proposed filter, a nonreciprocal BPF at 1.46 GHz was designed and fabricated on Taconic substrate with a dielectric constant of 2.2 and thickness

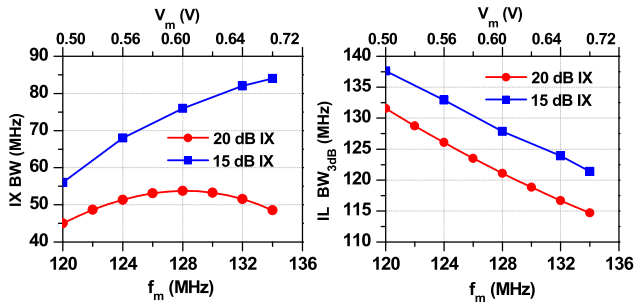


Fig. 5. Simulated 3-dB forward IL and reverse isolation BWs according to f_m and V_m .

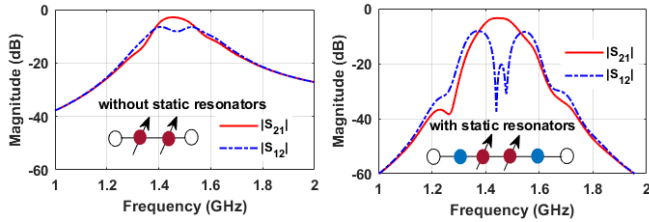


Fig. 6. Simulation results of nonreciprocal BPF with and without static resonators.

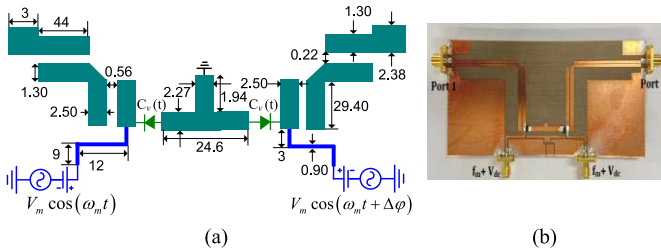


Fig. 7. (a) Physical layout with dimensions and (b) photograph of fabricated nonreciprocal BPF. Physical dimensions in millimeter (mm).

of 0.78 mm. Fig. 7 presents the physical layout, as well as a photograph, of the fabricated filter. The simulation was performed using ANSYS high frequency structure simulator (HFSS) and PathWave Advanced Design System (ADS) in conjunction with a large signal scattering analysis module. The time-varying capacitor was implemented by modulating varactor SMV-1233-079LF.

Fig. 8(a) shows the simulated and measured reciprocal responses. The reverse-biased dc voltage of 1.52 V was applied to two varactors. Without modulation, the filter exhibited a reciprocal response with IL of 1.90 dB at 1.46 GHz and RL better than 15 dB.

According to the previously described parametric studies, the modulation parameters of $f_m = 125$ MHz, $\Delta\phi = 65^\circ$, and $V_m = 0.7$ V allow for nonreciprocal BPF response. Fig. 8(b) shows the simulation and measurement results of the nonreciprocal BPF. Notably, the measurement and simulation results are consistent with each other. The measured forward IL ($|S_{21}|$) was 3.10 dB at 1.46 GHz, which is 1.20 dB higher than in the static case. This is attributable to power conversion to the intermodulation frequencies [12]. Likewise, the measured reverse isolation ($|S_{12}|$) was 20.2 dB at 1.46 GHz and had two poles providing 20-dB backward isolation of 50 MHz. The input and output RLs were better than 15.2 dB within 20-dB isolation BW.

Table II compares the performances of the proposed nonreciprocal BPF with state-of-arts. Simpson *et al.* [12], [13]

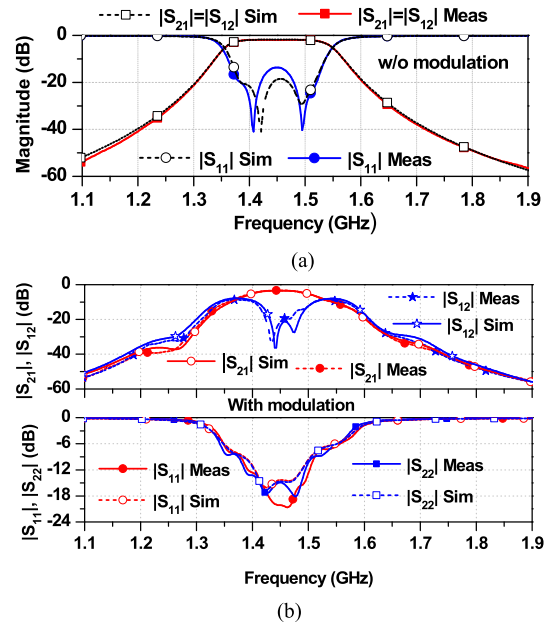


Fig. 8. Simulation and measurement results. (a) Nonmodulated reciprocal response and (b) modulated nonreciprocal response.

TABLE II
COMPARISON BETWEEN THIS WORK AND STATE-OF-ARTS

	[11]	[12]	[14]	[15]	[16]	This work
f_0 (GHz)	0.19	0.143	0.96	1	1.02	1.46
TVR	3	3	3	3	2	2
IL (dB)	1.50	3.70	4.5	3.90	5.50	3.10
Δ IL (dB)	NA	NA	1.7	1.30	2.80	1.20
RL (dB)	15	14	NA	16.1	12	15.2
IX @ f_0 (dB)	20.2	34.8	18.3	23.2	11.7	20.2
BW _{IX} (MHz)	20	NA	NA	42	NA	50
IX poles	2	1	2	2	1	2

TVR: Number of time-modulated resonators. IL: forward insertion loss ($|S_{21}|$). Δ IL: insertion loss degradation due to modulation. IX @ f_0 : backward reverse isolation ($|S_{12}|$), BW_{IX}: 20-dB reverse isolation bandwidth, IX poles: number of poles in reverse isolation.

reported a lumped element nonreciprocal BPF that used three time-modulated resonators, while Wu *et al.* [15] reported a similar microstrip line nonreciprocal BPF with complicated modulation circuit that lead higher IL. To create two poles in reverse isolation ($|S_{12}|$), Simpson *et al.* [12], [13], Alvarez Melcon *et al.* [14], and Wu *et al.* [15], [16] required at least three time-modulated resonators design that increases modulation circuit complexity. In this work, in contrast, developed a nonreciprocal BPF that relies on simplified and more efficient modulation circuit that required a fewer time-modulated resonators to achieve wideband and high reverse isolation.

IV. CONCLUSION

This letter demonstrated a microstrip line nonreciprocal BPF using coupled static and time-modulated resonators. This design requires fewer time-modulated resonators to create two poles in reverse isolation than alternative designs, thereby simplifying the modulation signal circuit. To experimentally validate the design, a nonreciprocal BPF at center frequency of 1.46 GHz was designed and fabricated. The proposed filter performs nonreciprocal filtering well, and does so with less time-modulated modulation resonators.

REFERENCES

- [1] S. Hong *et al.*, "Application of self-interference cancellation in 5G and beyond," *IEEE Commun. Mag.*, vol. 52, no. 2, pp. 114–121, Feb. 2014, doi: [10.1109/MCOM.2014.6736751](https://doi.org/10.1109/MCOM.2014.6736751).
- [2] N. Reiskarimian, A. Nagulu, T. Dinc, and H. Krishnaswamy, "Nonreciprocal electronic devices: A hypothesis turned into reality," *IEEE Microw. Mag.*, vol. 20, no. 4, pp. 94–111, Apr. 2019, doi: [10.1109/MMM.2019.2891380](https://doi.org/10.1109/MMM.2019.2891380).
- [3] J. Zhou *et al.*, "Integrated full duplex radios," *IEEE Commun. Mag.*, vol. 55, no. 4, pp. 142–151, Apr. 2017, doi: [10.1109/MCOM.2017.1600583](https://doi.org/10.1109/MCOM.2017.1600583).
- [4] C. E. Fay and R. L. Comstock, "Operation of the ferrite junction circulator," *IEEE Trans. Microw. Theory Techn.*, vol. MTT-13, no. 1, pp. 15–27, Jan. 1965, doi: [10.1109/TMTT.1965.1125923](https://doi.org/10.1109/TMTT.1965.1125923).
- [5] C. K. Seewald and J. R. Bray, "Ferrite-filled antisymmetrically biased rectangular waveguide isolator using magnetostatic surface wave modes," *IEEE Trans. Microw. Theory Techn.*, vol. 58, no. 6, pp. 1493–1501, Jun. 2010, doi: [10.1109/TMTT.2010.2047919](https://doi.org/10.1109/TMTT.2010.2047919).
- [6] T. Kodera, D. L. Sounas, and C. Caloz, "Magnetless nonreciprocal metamaterial (MNM) technology: Application to microwave components," *IEEE Trans. Microw. Theory Techn.*, vol. 61, no. 3, pp. 1030–1042, Mar. 2013, doi: [10.1109/TMTT.2013.2238246](https://doi.org/10.1109/TMTT.2013.2238246).
- [7] C. Caloz, A. Alù, S. Tretyakov, D. Sounas, K. Achouri, and Z.-L. Deck-Léger, "Electromagnetic nonreciprocity," *Phys. Rev. Appl.*, vol. 10, no. 4, Oct. 2018, Art. no. 047001, doi: [10.1103/PhysRevApplied.10.047001](https://doi.org/10.1103/PhysRevApplied.10.047001).
- [8] N. A. Estep, D. L. Sounas, and A. Alù, "Magnetless microwave circulators based on spatiotemporally modulated rings of coupled resonators," *IEEE Trans. Microw. Theory Techn.*, vol. 64, no. 2, pp. 502–518, Feb. 2016, doi: [10.1109/TMTT.2015.2511737](https://doi.org/10.1109/TMTT.2015.2511737).
- [9] A. Kord, D. L. Sounas, Z. Xiao, and A. Alu, "Broadband cyclic-symmetric magnetless circulators and theoretical bounds on their bandwidth," *IEEE Trans. Microw. Theory Techn.*, vol. 66, no. 12, pp. 5472–5481, Dec. 2018, doi: [10.1109/TMTT.2018.2860023](https://doi.org/10.1109/TMTT.2018.2860023).
- [10] A. Kord, D. L. Sounas, and A. Alù, "Pseudo-linear time-invariant magnetless circulators based on differential spatiotemporal modulation of resonant junctions," *IEEE Trans. Microw. Theory Techn.*, vol. 66, no. 6, pp. 2731–2745, Jun. 2018, doi: [10.1109/TMTT.2018.2818152](https://doi.org/10.1109/TMTT.2018.2818152).
- [11] X. Wu *et al.*, "Isolating bandpass filters using time-modulated resonators," *IEEE Trans. Microw. Theory Techn.*, vol. 67, no. 6, pp. 2331–2345, Apr. 2019, doi: [10.1109/TMTT.2019.2908868](https://doi.org/10.1109/TMTT.2019.2908868).
- [12] D. Simpson and D. Psychogiou, "Magnet-less non-reciprocal bandpass filters with tunable center frequency," in *Proc. 49th Eur. Microw. Conf. (EuMC)*, Oct. 2019, pp. 460–463, doi: [10.23919/EuMC.2019.8910732](https://doi.org/10.23919/EuMC.2019.8910732).
- [13] D. Simpson and D. Psychogiou, "Fully-reconfigurable non-reciprocal bandpass filters," in *IEEE MTT-S Int. Microw. Symp. Dig.*, Aug. 2020, pp. 807–810, doi: [10.1109/IMS30576.2020.9224096](https://doi.org/10.1109/IMS30576.2020.9224096).
- [14] A. Alvarez-Melcon, X. Wu, J. Zang, X. Liu, and J. S. Gomez-Diaz, "Coupling matrix representation of nonreciprocal filters based on time-modulated resonators," *IEEE Trans. Microw. Theory Techn.*, vol. 67, no. 12, pp. 4751–4763, Dec. 2019, doi: [10.1109/TMTT.2019.2945756](https://doi.org/10.1109/TMTT.2019.2945756).
- [15] X. Wu, M. Nafe, A. Alvarez Melcon, J. S. Gómez-Díaz, and X. Liu, "Frequency tunable non-reciprocal bandpass filter using time-modulated microstrip $\lambda_g/2$ resonators," *IEEE Trans. Circuits Syst. II, Exp. Briefs*, vol. 68, no. 2, pp. 667–671, Feb. 2021.
- [16] X. Wu, M. Nafe, A. A. Melcón, J. S. Gómez-Díaz, and X. Liu, "A non-reciprocal microstrip bandpass filter based on spatio-temporal modulation," in *IEEE MTT-S Int. Microw. Symp. Dig.*, Jun. 2019, pp. 9–12, doi: [10.1109/MWSYM.2019.8700732](https://doi.org/10.1109/MWSYM.2019.8700732).
- [17] X. Wu, M. Nafe, and X. Liu, "Non-reciprocal 2nd-order bandpass filter by using time-modulated microstrip quarter-wavelength resonators," in *Proc. Int. Conf. Microw. Millim. Wave Technol. (ICMMT)*, May 2019, pp. 1–3.
- [18] X. Wu, M. Nafe, and X. Liu, "A magnetless microstrip filtering circulator based on coupled static and time-modulated resonators," in *IEEE MTT-S Int. Microw. Symp. Dig.*, Aug. 2020, pp. 948–951.
- [19] *SMV123x Series: Hyper-Abrupt Junction Tuning Varactors*, Skyworks Solutions, Irvine, CA, USA, Nov. 2018.